analytical chemistry

pubs.acs.org/ac Article

How Choice of Model Membrane Affects Protein−Glycosphingolipid Interactions: Insights from Native Mass Spectrometry

Ling Han, Linh Nguyen, Edward N. Schmidt, Mansoore Esmaili, Elena N. Kitova, Michael Overduin, Matthew S. Macauley, and John S. Klassen*

Cite This: https://doi.org/10.1021/acs.analchem.2c03067 Read Online

ACCESS | Metrics & More | Article Recommendations | Supporting Information

ABSTRACT: Interactions between glycan-binding proteins (GBPs) and glycosphingolipids (GSLs) are involved in numerous physiological and pathophysiological processes. Many model membrane systems are available for studying GBP−GSL interactions, but a systematic investigation has not been carried out on how the nature of the model membrane affects binding. In this work, we use electrospray ionization mass spectrometry (ESI-MS), both direct and competitive assays, to measure the binding of cholera toxin B subunit homopentamer (CTB_5) to GM1 ganglioside in liposomes, bilayer islands [styrene maleic acid lipid particles (SMALPs), nanodiscs (NDs), and picodiscs (PDs)], and micelles. We find that direct ESI-MS analysis of CTB_5 binding to GM1 is unreliable due to non-uniform response factors, incomplete extraction of bound GM1 in the gas phase, and nonspecific CTB_5−GM1 interactions. Conversely, indirect proxy ligand ESI-MS measurements show that the intrinsic (per binding site) association constants of CTB_5 for PDs, NDs, and SMALPs are similar and comparable to the affinity of soluble GM1 pentasaccharide ($GM1_{os}$). The observed affinity decreases with increasing GM1 content due to molecular crowding stemming from GM1 clustering. Unlike the smaller model membranes, the observed affinity of CTB_5 toward GM1 liposomes is ∼10-fold weaker than $GM1_{os}$ and relatively insensitive to the GM1 content. GM1 glycomicelles exhibit the lowest affinity, ∼35-fold weaker than $GM1_{os}$. Together, the results highlight experimental design considerations for quantitative GBP−GSL binding studies involving multisubunit GBPs and factors to consider when comparing results obtained with different membrane systems. Notably, they suggest that bilayer islands with a low percentage of GSL, wherein clustering is minimized, are ideal for assessing intrinsic strength of GBP−GSL interactions in a membrane environment, while binding to liposomes, which is sub-optimal due to extensive clustering, may be more representative of authentic cellular environments.

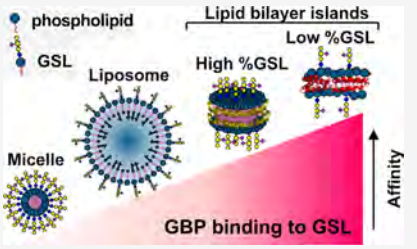

INTRODUCTION

Interactions between cell surface glycosphingolipids (GSLs) and glycan-binding proteins (GBPs) are implicated in many healthy (e.g., cellular recognition, adhesion, signal transduction, and trafficking) and pathophysiological processes (e.g., neurodegenerative and autoimmune diseases, cancer, and bacterial and viral infections).[1−4] GSLs are amphipathic molecules. The hydrophobic lipid moiety (ceramide) embeds into the cellular membrane, while the hydrophilic carbohydrate head group protrudes into the aqueous environment, making it accessible to GBPs. It is generally accepted that the nature of the lipid membrane environment can affect the kinetics and thermodynamics of GBP−GSL interactions.[5,6] For example, GSLs tend to cluster together in lipid bilayers via the formation of intermolecular hydrogen bonds between the saccharide head groups, making them less accessible for GBP binding. As a result, the apparent association constant (K_a) for binding to a GBP typically decreases with increasing GSL densities.[7,8] The presence of other components in the membrane may also modulate binding. Cholesterol, a major component of cell membranes (∼30% of the total lipid composition in lipid rafts) that is important for maintaining the membrane rigidity, has been shown to affect GSL binding.[9] While the origin of this effect has not been conclusively established, it might be due to GSL "masking," whereby interaction between cholesterol and the GSL ceramide moiety induces (carbohydrate) conformational changes that in turn alter GBP binding,[10,11] or to cholesterol's ability to increase the order of lipid packing.[12−14] Relatedly, the nature of the GSL ceramide group has also been shown to influence cell binding and trafficking of GBPs.[15]

The potential influence of the membrane environment and composition on GBP−GSL binding properties raises important considerations when designing the experimental setup for quantitative binding studies and comparing data measured with different assays and experimental conditions. While some investigations into GBP−GSL binding are performed in the absence of a membrane environment, wherein the GSL is

Received: July 15, 2022
Accepted: October 24, 2022

immobilized on a surface (e.g., enzyme-linked immunosorbent assay or glycan array), most employ model (artificial) membranes in which GSLs are incorporated. Depending on their structure, model membrane systems can be classified into three main categories: (i) planar supported bilayers (supported lipid bilayers), (ii) monolayer (e.g., micelles) or bilayer vesicles (e.g., liposomes), and (iii) bilayer islands [e.g., nanodiscs (NDs), picodiscs (PDs), and styrene maleic acid lipid particles (SMALPs)].[16]

Supported lipid bilayers are two-dimensional thin film coatings composed of phospholipid bilayer attached to an underlying solid surface. They can mimic the asymmetric distribution of lipids between the two leaflets, as found in biological membranes, although the presence of the underlying solid substrate may reduce lateral diffusion within the membrane.[17] Supported lipid bilayers can be easily integrated with surface-based (surface-sensitive) assays, such as surface plasmon resonance spectroscopy, fluorescence microscopy, and quartz crystal microbalance,[17] and have been extensively used to study GBP−GSL-binding kinetics and energetics.[18,19] However, they are generally incompatible with in-solution binding assays, such as isothermal titration calorimetry, nuclear magnetic resonance spectroscopy, and electrospray ionization mass spectrometry (ESI-MS), which measure binding thermodynamics and stoichiometry.

Mono- and bilayer vesicles and bilayer islands are generally compatible with in-solution binding assays[20] and are commonly used to study GBP−GSL interactions.[21−23] A graphic representation of these model membranes and their size distributions are shown in Figure 1a. Normal-phase micelles are closed lipid monolayers with a hydrophobic core and polar surface.[24] GSLs are known to spontaneous assemble into glycomicelles in aqueous solution at concentrations above the critical micelle concentration. For example, the ganglioside GM1, which has a critical micelle concentration of ∼20 nM,

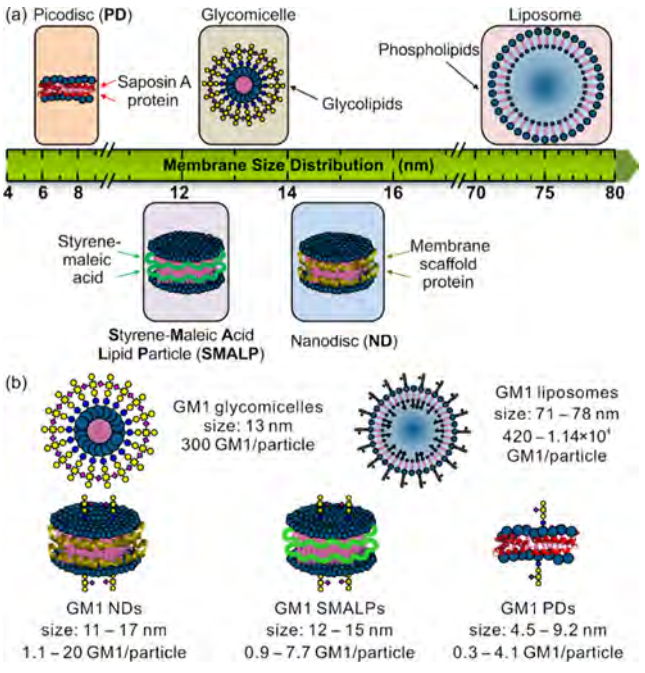

Figure 1. (a) Illustration of the architecture and size of common model membranes. (b) Characteristics of the GM1-containing model membranes used in the present study.

forms glycomicelles with diameters in the range of 10 to 30 nm and molecular weights (MWs) of between 300 and 500 kDa.[25] Liposomes, which have an aqueous core surrounded by two lipid leaflets and resemble native cell membranes, are the most popular model membrane system. Liposomal membranes are composed of phospholipids (e.g., phosphatidylcholine) and can incorporate steroids (e.g., cholesterol) and GSLs.[26] Small unilamellar liposomes, which have single phospholipid bilayer sphere enclosing the aqueous solution and diameters of ∼100 nm have been used to study GBP−GSL binding using gel filtration, tryptophan fluorescence, and circular dichroism spectroscopy.[27] Additionally, large unilamellar liposomes have been used for liposome microarray screening against GBPs.[28]

Unlike micelles and liposomes, bilayer islands are planar lipid bilayer systems. NDs, the most widely used bilayer islands, are discoidal phospholipid bilayers surrounded by two copies of the membrane scaffold protein.[23] The size of an ND depends on the choice of the membrane scaffold protein (for MSP1E1 consisting of ∼200 lipids, diameter ∼10 nm, and MW ∼150 kDa).[29] SMALPs (∼80−100 kDa) are structurally similar to NDs, except that a styrene−maleic acid copolymer is used in place of a membrane scaffold protein.[30] PDs are composed of human sphingolipid activator protein saposin A (SapA) and a small number of phospholipids (11 ± 2 lipid molecules per SapA).[31] At neutral pH, PDs consist predominantly of three SapA, with a MW ∼50 kDa and diameter of ∼3 nm.[31]

Because of differences in size and shape, lipid and GSL composition, and polydispersity, the nature of the membrane system has a strong possibility to influence GBP−GSL interactions. However, to the best of our knowledge, model membrane-specific effects in GBP−GSL binding measurements have not been systematically studied. Here, we investigate how the choice of model membrane influences the strength of GSL binding with a soluble GBP. Interactions between GM1, displayed in five different model membranes (glycomicelles, small unilamellar liposomes, NDs, SMALPs, and PDs) at varying percentages of total lipid, and the cholera toxin B subunit homopentamer (CTB_5) were quantified using direct ESI-MS and the proxy ligand ESI-MS assay.[12,32] Comparison of the results highlights important experimental design considerations for quantitative GBP−GSL binding studies involving multisubunit GBPs and GSL-containing model membranes and factors to consider when comparing results obtained with different membrane systems.

EXPERIMENTAL SECTION

Materials and Methods. *Proteins, Styrene Maleic Acid Copolymers, Lipids, and Oligosaccharides.* CTB_5 (MW 58,040 Da) from *Vibrio cholerae* was purchased from Sigma-Aldrich Canada (Oakville, Canada). The recombinant MSP1E1 (MW 27,494 Da) was produced from the plasmid pMSP1E1 (Addgene, Cambridge, MA) and purified based on a procedure described elsewhere.[29] The SapA was a gift from Prof. G. Privé (University of Toronto). The SMALPs were assembled using styrene maleic acid copolymer SMA2000, which was prepared from styrene-maleic anhydride copolymer (TOTAL Cray Valley, Exton, PA) using base-catalyzed hydrolysis. The phospholipid 1-palmitoyl-2-oleoyl-sn-glycero-3-phosphocholine (POPC) was purchased from Avanti Polar Lipids (Alabaster, AL). The ganglioside GM1 and *N*-ω-CD3-octadecanoyl monosialoganglioside GM1 (GM1-d3) were purchased form Matreya LLC (State College, PA). The

https://doi.org/10.1021/acs.analchem.2c03067
Anal. Chem. XXXX, XXX, XXX−XXX

Table 1. Overview of GM1-Containing Model Membranes Used in the Present Study[a]

model membrane[b]	diameter (nm)	GM1 incorporation efficiency	average number of GM1 (per membrane)	K_a ($\times 10^6$ M^{-1})
0.5% GM1 ND	11.1 ± 2.1	1.05 ± 0.03[c]	1.05 ± 0.03[c]	1.5 ± 0.3[c]
1% GM1 ND	11.6 ± 1.3	0.98 ± 0.03[c]	1.96 ± 0.06[c]	1.1 ± 0.4[c]
5% GM1 ND	12.8 ± 2.0	0.57 ± 0.02[c]	5.7 ± 0.2[c]	0.56 ± 0.18[c]
10% GM1 ND	15.6 ± 2.8	0.77 ± 0.03[c]	15.4 ± 0.6[c]	0.47 ± 0.07[c]
15% GM1 ND	17.1 ± 3.0	0.67 ± 0.04[c]	20.1 ± 1.2[c]	0.35 ± 0.09[c]
2% GM1 PD	4.5 ± 2.8	0.55 ± 0.01	0.33 ± 0.01[d]	2.3 ± 0.1
5% GM1 PD	5.7 ± 1.2	0.51 ± 0.01	0.77 ± 0.02[d]	2.9 ± 0.4
10% GM1 PD	9.2 ± 1.4	0.66 ± 0.01	1.98 ± 0.03[d]	1.6 ±0.1
20% GM1 PD	6.8 ± 1.4	0.69 ± 0.04	4.13 ± 0.25[d]	0.96 ± 0.03
1% GM1 SMALP	11.8 ± 2.4	NA[e]	0.93 ± 0.06[f]	1.1 ± 0.1
5% GM1 SMALP	11.9 ± 2.1	NA[e]	3.73 ± 0.28[f]	0.62 ± 0.04
10% GM1 SMALP	14.7 ± 2.6	NA[e]	7.74 ± 0.39[f]	0.46 ± 0.03
1% GM1 liposome	75 ± 26	0.96 ± 0.08	420 ± 35[g]	0.43 ± 0.01[g]
3% GM1 liposome	78 ± 36	0.96 ± 0.06	1365 ± 90[g]	0.56 ± 0.07[g]
10% GM1 liposome	76 ± 27	0.93 ± 0.03	4181 ± 140[g]	0.28 ± 0.02[g]
30% GM1 liposome	71 ± 32	0.98 ± 0.06	11444 ± 732[g]	0.28 ± 0.01[g]
GM1 glycomicelle	13 ± 3	NA[e]	300 ± 54[h]	0.09 ± 0.01

[a]Size, determined by DLS, GM1 incorporation efficiency, average number of GM1 per membrane particle, and the intrinsic association constant (K_a) of GM1 for CTB_5 measured in aqueous ammonium acetate (200 mM, pH 6.8 and 25 °C) using the proxy ligand ESI-MS assay. Uncertainties correspond to one standard deviation. [b]Percentages calculated from the molar ratio of GM1 and phospholipid used for membrane preparation. [c]Values adapted from ref 12. [d]Calculated assuming each PD consists of three SapA. [e]Not applicable ≡ NA. [f]Calculated assuming each SMALP consists of 25 kDa SMA copolymer. [g]Calculated based on the size of (71−78 nm in diameter) and total lipid number (3.9×10^4 to 4.7×10^4) of the liposomes, assuming 57% of GM1 present in the outer leaflet of the liposomes. Storage of the liposomes (at 4 °C) was found to lead to only minor changes in sizes (≤2.3% over 1 month). [h]Calculated based on assumption that the glycomicelle consists of 300 GM1.

GM1 pentasaccharide ($GM1_{os}$) was purchased from Elicityl SA (Crolles, France). The structures of the lipids and oligosaccharide are shown in Figure S1. More details about the stock solution preparation can be found in the Supporting Information.

Preparation of the GM1-Containing Model Membranes. A detailed description of the procedures used to prepare the GM1-containing NDs, PDs, SMALPs, liposomes, and glycomicelles and the method for quantifying the GM1 content in these model membranes are described in the Supporting Information.[12,30,31,33]

Dynamic Light Scattering. Dynamic light scattering (DLS), performed using a Zetasizer Nano S instrument (Malvern Panalytical Ltd., Malvern, UK), was used to evaluate the average sizes of the model membranes used in the current study. Unless otherwise specified, each sample was diluted in ammonium acetate (200 mM, pH 6.8, 25 °C) to 100 μM (total lipid concentration) and then loaded into a disposable DLS cuvette for analysis.

Electrospray Ionization Mass Spectrometry. All ESI-MS measurements were carried out using a Synapt G2S quadrupole-ion mobility separation-time of flight (Q-IMS-TOF) mass spectrometer (Waters, Manchester, UK) equipped with a nanoflow ESI (nanoESI) source. The binding measurements were performed in the positive ion mode, whereas the quantification of the GM1 content was performed in the negative ion mode. Details of experimental and instrumental parameters used and data analysis procedures are provided in the Supporting Information.

ESI-MS Binding Measurements. The fraction of occupied binding sites (F) and apparent association constant ($K_{a,app}$) for CTB_5 binding to GM1-containing model membranes was measured directly by ESI-MS.[32,33] The intrinsic association constant (K_a) was quantified using the proxy ligand ESI-MS method, which was performed using the GM1 pentasaccharide ($GM1_{os}$) as the proxy ligand. A detailed description of the assay and data analysis procedures is given in the Supporting Information and can be found elsewhere.[12,32,34]

RESULTS AND DISCUSSION

GM1-Containing Model Membranes. Binding measurements were performed on CTB_5 and GM1 incorporated into glycomicelles, liposomes, NDs, SMALPs, and PDs. The relative sizes and average GM1 content of these model membranes are summarized in Figure 1b and Table 1. With the exception of the glycomicelles, the percentage of GM1 in each membrane system varied in an effort to delineate the influence of the nature of the model membrane from GM1 content on binding. The average number of GM1 (per membrane particle) in a given sample was measured by ESI-MS using a stable isotope internal standard method, which is described in the Supporting Information and elsewhere.[12] Additional information on the characterization of the model membranes is given in the Supporting Information, and representative mass spectra of the NDs, SMALPs, and PDs are shown in Figures S2−S4.

CTB_5 Interactions with GM1-Containing Model Membranes. *Direct ESI-MS Measurements.* It was previously shown that GBP−GSL complexes can be directly detected by ESI-MS analysis of aqueous solutions of GBP and GSL-containing NDs and PDs or GM1 glycomicelles.[31−33] The GBP−GSL complex ions detected are believed to originate in solution from specific interactions with GSLs in the model membrane. Intact GBP−GSL complexes spontaneously detach from the membrane during the ESI process (or in the gas phase) as a result of Coulombic repulsion between the GBP and the membrane. However, the relative abundances of free and GSL-bound GBP ions do not necessarily reflect solution concentrations and, in the case of glycomicelles, the measurements can produce false positives (nonspecific interactions originating during the ESI process) and false negatives (loss of specific interactions originally present in solution).[33] To more

https://doi.org/10.1021/acs.analchem.2c03067
Anal. Chem. XXXX, XXX, XXX−XXX

fully assess the strengths and limitations of direct ESI-MS analysis, binding measurements were performed, in a titration format, on each membrane system. Due to the inherent heterogeneity of the model membranes and signal overlap with CTB_5–GM1 complex ions, IMS was used to separate signals corresponding to the CTB_5–GM1 complexes from those of the model membranes.[31] Through the application of IMS, the contribution of the membrane ions to the CTB_5 signal was efficiently filtered out, enabling the abundances of free and GM1-bound bound CTB_5 species to be determined directly from the ESI mass spectra.

Inspection of the mass spectra (Figures 2 and S5–S8) reveals several general features. At low concentrations of low % GM1 membranes (<10%), ion signal corresponding to free CTB_5 dominates (Figures S5a,c, S6a,c, S7a–c, and S8a–c). This observation likely reflects the low ESI-MS response factors of the CTB_5–GM1 complex ions, which are released from the model membrane during ESI or in the gas phase, relative to those of free CTB_5 ions, which originate directly from solution.[32,35] At higher concentrations, ligand binding to CTB_5 is observed, and binding site occupancy increases with GM1 concentration, reaching a maximum value of ∼90% (Figure S9). As discussed elsewhere, this observation likely reflects the incomplete extraction of GM1 (bound to CTB_5) from the membrane in the gas phase.[32]

At low concentrations of high %GM1 membranes, free CTB_5 ion signal dominated the mass spectra (Figures 2a, S5g, S8e, and g). At elevated concentrations, ions corresponding to CTB_5 bound to up to 6 GM1 were detected (Figures 2c,d, S5e–h, and S6i,j). As CTB_5 possesses only five GM1 binding sites,[36] these results indicate a propensity for CTB_5 to form nonspecific interactions with GM1 (when bound to the membrane) during the ESI process. The occurrence of nonspecific binding obscures the true binding stoichiometry and affinity.[37] Curiously, at intermediate concentrations, no CTB_5 (free or bound) ion signal was observed (Figure 2b). To the best of our knowledge, this phenomenon has not been previously reported. While the exact reason for signal suppression is not fully understood, it may be due to binding of CTB_5 to multiple particles in solution, leading to the formation of large aggregates (Figure 3a). The combined effects of the low ESI response factors of these particles and, possibly, low release efficiencies, together with the low abundance of free CTB_5 in solution would account for the

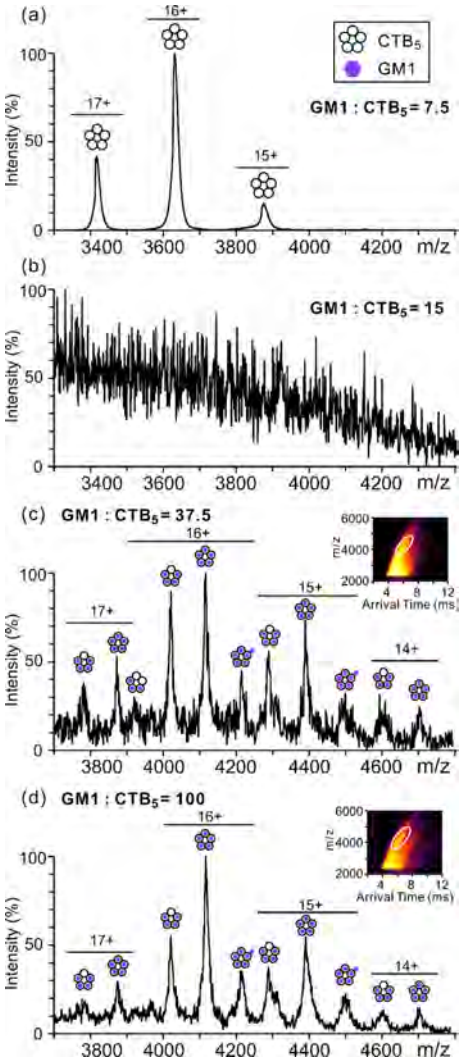

Figure 2. CTB_5 binding to GM1 glycomicelles. Representative ESI mass spectra acquired in the positive ion mode for aqueous ammonium acetate solutions (200 mM, 25 °C and pH 6.8) of CTB_5 (4 μM) with (a) 30, (b) 60, (c) 150, and (d) 400 μM GM1 glycomicelles. Five-petal icon represents CTB_5, and purple hexagon represents GM1. Mass spectra in (c,d) were generated from the region denoted in the IMS heat map (inset).

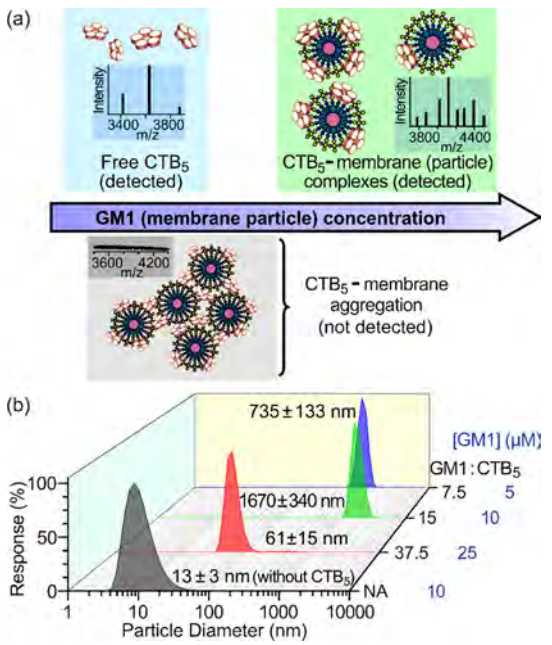

Figure 3. (a) Influence of stoichiometry (CTB_5 and high % GM1-containing model membranes) on ESI-MS detection of free and GM1-bound CTB_5 species. High (relative) CTB_5 concentration: both free and GM1-bound CTB_5 species present in solution. The free CTB_5 is detectable, while the GM1-bound CTB_5, which interacts with GM1 in multiple membranes, is undetectable. Similar CTB_5 and membrane concentrations: no free CTB_5 in solution; GM1-bound CTB_5 interacts with GM1 in multiple membranes and is undetectable. Low (relative) CTB_5 concentration: no free CTB_5 in solution; GM1-bound CTB_5 interacts predominantly with GM1 in a single membrane particle and is detectable. (b) Particle size distributions determined by DLS for a GM1 glycomicelle solution (10 μM GM1); and solutions of CTB_5 (0.67 μM) and GM1 glycomicelle (corresponding to 25, 10, and 5 μM GM1). Not applicable ≡ NA.

https://doi.org/10.1021/acs.analchem.2c03067
Anal. Chem. XXXX, XXX, XXX–XXX

loss of CTB_5 signal. Below is a brief summary of the key findings for each of the model membranes.

Glycomicelles. For the GM1 glycomicelle solutions (Figure 2), only free CTB_5 ions were detected at GM1 concentrations ≤40 μM (Figure 2a). CTB_5−GM1 complex ions were detectable (Figures 2c,d) at GM1 concentrations between 80 and 400 μM (the highest concentration tested), which correspond to glycomicelle concentrations of 0.27 and 1.33 μM, respectively. The complexes detected consisted predominantly of CTB_5 bound to 4 or 5 GM1. However, ions corresponding to six bound GM1, which points to the occurrence of nonspecific binding, were also observed (Figures 2c,d). Notably, the CTB_5 signal was almost completely suppressed at GM1 concentrations between 40 and 80 μM (Figure 2b). As described above, this phenomenon is suggested to arise from CTB_5−GM1 glycomicelle aggregation (Figure 3a). To support this hypothesis, DLS analysis was performed on solutions of CTB_5 (fixed concentration) and GM1 glycomicelle (variable concentration). As shown in Figure 3b, large particles, with diameters in the μm range, were detected in solutions with GM1 concentrations of 5 ($GM1/CTB_5$ = 7.5) and 10 μM ($GM1/CTB_5$ = 15). ESI-MS analysis of solutions with comparable $GM1/CTB_5$ ratios failed to detect any ion signal corresponding to CTB_5−GM1 complexes (Figure 2a,b), and free CTB_5 was only observed at the lowest ratio (Figure 2a). At higher GM1 concentrations ($GM1/CTB_5$ = 37.5), smaller diameter (~60 nm) particles were detected. For solutions of comparable (or higher) $GM1/CTB_5$ ratios, CTB_5−GM1 complexes were detected by ESI-MS (Figure 2c,d). Their appearance is presumably due to higher relative response factors compared to the larger aggregates. Interestingly, the additional GM1 to solutions with initially low $GM1/CTB_5$ ratios leads to the disappearance of the larger (μm) diameter particles and the appearance of the smaller ones (data not shown). This finding suggests that the aggregation process is reversible. As discussed below, this phenomenon is observed for other model membranes and appears to be general.

GM1 Liposomes. Analysis of solutions of CTB_5 and liposomes prepared with 1 and 3% GM1 revealed sequential binding of up to 5 GM1 with increasing liposome concentrations (Figure S5a−d). However, for liposomes with high % GM1 (10 and 30%), the binding data resemble those acquired for the glycomicelles. Only free CTB_5 was observed at ≤12 μM GM1 for 10% GM1 liposome (corresponding to 4.8 nM liposome, Figure S9d) and ≤28 μM GM1 for 30% GM1 liposome (corresponding to 4.4 nM liposome, Figure S9e). At higher GM1 concentrations, CTB_5 binding to 3−6 GM1 was observed (Figure S5e−h). For 30% GM1 liposome, all CTB_5 ion signals were suppressed between 35 μM and 64 μM GM1 (5.2−9.6 nM liposomes).

GM1 NDs. Sequential binding of GM1 to CTB_5 was observed with the 0.5−10% GM1 NDs (Figure S6a −h). The results obtained with the 15% GM1 NDs are similar to those observed for 30% GM1 liposome and GM1 glycomicelles. Free CTB_5 ions were observed at ≤20 μM GM1 (Figure S9h), while [CTB_5 + (3−5) GM1] complex ions were detected at GM1 concentrations ≥33 μM (corresponding to 1.6 μM ND, Figure S6i). At higher concentrations (e.g., [GM1] ≥145 μM, equivalent to 7.3 μM ND, Figure S6j), the signal corresponding to (CTB_5 + 6 GM1) complex ions was also detected.

GM1 SMALPs. Overall, GM1-containing SMALPs yielded binding data similar to those obtained from NDs with comparable GM1 content (Figure S7). For example, CTB_5 bound to up to 3 GM1 was detected for 1% GM1 SMALP (Figure S7a,b). Despite the uniformly low-ion signals detected, the binding observed for 5 and 10% GM1 SMALPs was similar to that of the corresponding NDs (Figure S7c−f). However, due to the pronounced background noise arising from the SMA polymer, ESI-MS detection of the CTB_5−GM1 complex ions using SMALPs was challenging, even with the use of IMS.

GM1 PDs. At the highest concentrations of GM1 PDs tested (2 and 5%), only partial binding site occupancy was achieved—between 0 and 3 bound GM1 for 2% GM1 PD; 1 to 5 GM1 for 5% GM1 PD (Figures S8a−d). In contrast, 4−5 GM1-bound CTB_5 ions were the major species detected for 10 and 20% GM1 PDs at high concentrations, which is similar to the cases of ND containing low % GM1 (Figure S8e−h).

Apparent Affinities. For each membrane system, the concentration-dependent fractional occupancy (F) of CTB_5-binding sites was calculated (eq S5). Representative plots of F versus GM1 concentration (based on the GM1 content established for each membrane sample) are shown in Figure S9. F was negligibly small in the low concentration portion of the binding isotherms, presumably due to the non-uniform response factors of free CTB_5 (directly produced from solution) and the CTB_5−GM1 complex (released from the membrane in the gas-phase) ions. At the highest GM1 concentrations analyzed, F reaches a limiting value of ~90% occupancy, which is attributed to incomplete extraction of GM1 from the membrane in the gas phase.[32]

Although the titration data cannot be fully described by a simple 1:1 model (eq S6), it was fit to the portion of the titration curves corresponding to the data for which no free CTB_5 was observed (F > 0.5) to estimate $K_{a,app}$ (Figure S9, Table S1). Notably, the $K_{a,app}$ determined for the 5−20% GM1 PDs and 5−10% GM1 SMALPs, which range from 1.2×10^6 to 2.7×10^6 M^{-1}, is similar to the reported intrinsic (per binding site and in the absence of cooperativity) affinity of $GM1_{os}$ [$(3.2 \pm 0.2) \times 10^6$ M^{-1}].[38] The $K_{a,app}$ for the 1% GM1 ND (1.6×10^6 M^{-1}) is of similar magnitude; the values for the higher % GM1 NDs are ~10^5 M^{-1}. For GM1 liposomes, it was assumed that ~57% lipids (and GM1) are in the outer leaflet, based on their diameter and the assumed thickness of the bilayer (5 nm).[39] Similar to the NDs, the $K_{a,app}$ measured for the liposomes decreases with the increasing %GM1 [from 1.1×10^6 M^{-1} (1%) to 1.4×10^5 M^{-1} (30%)]. The GM1 glycomicelles exhibit the lowest $K_{a,app}$ (4.1×10^4 M^{-1}). Interestingly, the membranes containing high %GM1 (e.g., 15% GM1 ND, 30% GM1 liposome, and GM1 glycomicelles) all had significantly weaker affinities compared to the low % GM1 counterparts. No $K_{a,app}$ determination was possible for 1% GM1 SMALP (Figure S9i) or 2% GM1 PD (Figure S9l) due to the low occupancy at the highest membrane concentrations tested.

The results of this analysis demonstrate that direct ESI-MS analysis of CTB_5 binding to GM1 in model membranes is unreliable. Due to non-uniform response factors, the distribution of free and GM1-bound CTB_5 in solution is not generally reflected in the relative abundances of the corresponding gaseous ions. ESI-MS analysis can provide an estimate of the relative occupancy of CTB_5-binding sites, due to the similarity in response factors. However, incomplete extraction of bound GM1 (by CTB_5) in the gas phase, which was observed for all of the model membranes tested, and the occurrence of nonspecific CTB_5−GM1 binding at high GM1

https://doi.org/10.1021/acs.analchem.2c03067
Anal. Chem. XXXX, XXX, XXX−XXX

concentrations represent significant sources of error. Together, these results caution against the use of direct ESI-MS measurements performed using model membranes to quantify GBP−GSL binding.

Proxy Ligand ESI-MS. The proxy ligand ESI-MS method, a competitive ligand binding assay, was used to measure the affinities of GM1-containing model membranes for CTB_5.[12,32,34] The $GM1_{os}$ served as the proxy ligand (L_{proxy}).[38] Briefly, the intrinsic association constant (K_a), which describes the initial GM1 binding step, was quantified from changes in the abundance ratio of CTB_5 bound to 5 and 4 $GM1_{os}$ ($R_{proxy,5\text{-}4}$) measured by ESI-MS upon titration of the solution with a model membrane containing GM1.

Representative mass spectra acquired for CTB_5 and each model membrane, in the presence of L_{proxy}, are shown in Figure S10. In the absence of the model membrane, CTB_5 is predominantly bound to 4 and 5 $GM1_{os}$ {with the $R_{proxy,5\text{-}4}$ ratio ($[CTB_5 + 5GM1_{os}]/[CTB_5 + 4GM1_{os}]$) of 2.71 ± 0.02} under the solution conditions used (Figure S10a). In all cases, the addition of GM1-containing model membrane to solution resulted in a concentration-dependent increase in $R_{proxy,5\text{-}4}$, consistent with CTB_5 binding to the model membrane. Additionally, mixed CTB_5−$GM1_{os}$/GM1 species, consisting of 1 or 2 GM1, were detected, which is further evidence of CTB_5−GM1 binding. Proxy ligand assay was performed in a titration format, whereby the binding model (Scheme S1) was fit to the resulting titration curves (Figure S11). The intrinsic intermolecular GM1 affinity (K_a) determined for each sample is listed in Table 1 and shown in Figure 4a, and the major findings are summarized below.

GM1 NDs. The affinity of GM1-containing NDs, prepared with POPC, for CTB_5 has been previously measured using the proxy ligand ESI-MS method.[12] It was shown that, for NDs containing on average a single GM1 (0.5%), K_a [(1.5 ± 0.3) × 10^6 M^{-1}] is similar to that of free $GM1_{os}$ (Table 1).[12] This finding suggests that within the membrane and in the absence of other effects, the glycan moiety of GM1 is able to adopt a near optimal conformation for CTB_5 binding.[12] However, K_a decreases with increasing GM1 content of the ND sample (Table 1). A 4−5-fold decrease in affinity was observed for the NDs prepared with 15% GM1, which is the maximum percentage that can be used to prepare stable POPC NDs, is attributed to clustering of GM1 in the membrane, resulting from hydrogen bonding between the pentasaccharide moieties, which sterically hinders GM1 binding to CTB_5.[7,12,40] Notably, the K_a [(1.1−0.4) × 10^6 M^{-1}] is in reasonable agreement with $K_{a,app}$ estimated from the direct ESI-MS measurements for the 1−15% GM1 NDs (1.6 to 0.3 × 10^6 M^{-1}).

GM1 Liposomes. The K_a for liposomes, which ranges from 3 × 10^5 to 6 × 10^5 M^{-1}, is similar in magnitude to those measured for the high % GM1 (5−15%) NDs and SMALPs, vide infra, consistent with extensive clustering. However, unlike the NDs and SMALPs, the K_a measured for the liposomes does not exhibit a strong dependence on % GM1. This may be due to the large number of GM1 present in the liposomes, which promotes clustering even at low % GM1 (Table 1), such that the effects of clustering at higher percentages are less (relatively) significant. Indeed, according to the reported binding data obtained with supported lipid bilayers, CTB_5−GM1 affinities decrease ∼4-fold from 0.02 to 1% GM1 and an additional ∼2-fold from 1 to 10% GM1.[7] Interestingly, $K_{a,app}$ for 3−30% GM1 liposomes is similar to the measured K_a, while $K_{a,app}$ for 1% GM1 liposome [(1.1 ± 0.4) × 10^6 M^{-1}] is ∼3-fold larger.

GM1 Glycomicelles. Due to the ease of preparation, glycomicelles represent an attractive alternative to other model membranes for GBP−GSL binding studies. However, the K_a measured for the GM1 glycomicelles is >10-fold weaker than the values measured for 0.5% or 1% GM1 NDs (Table 1). The lower affinity is, perhaps, not surprising given that the glycomicelles are composed solely of GM1 (∼300 molecules). As a result, clustering is expected, resulting in non-optimal (for binding) presentation of the GM1 head group.[40]

GM1 SMALPs. The K_a measured for the SMALPs prepared with 1, 5, and 10% GM1 are similar to those measured for the NDs of similar composition (Table 1). The ∼2-fold decrease in K_a observed with increasing GM1 content is consistent with what is observed for NDs. These observations are not unexpected due to the size and structure similarities of NDs and SMAPLs. Surprisingly, though, $K_{a,app}$ for the 5 and 10% GM1 SMALPs are ∼3- and ∼6-fold larger than the corresponding K_a, respectively. These discrepancies are difficult to rationalize but may be related to the significant signal background observed with SMALPs, which introduces differential errors into the relative abundances of the free and bound GBP measured by ESI-MS.

GM1 PDs. The PDs exhibit the highest K_a in the range of 0.96 × 10^6 to 2.9 × 10^6 M^{-1} (Table 1). The highest affinity, which was obtained for 5% GM1 PD, closely resembles the value of $GM1_{os}$ affinities. Notably, the clustering effect is not as pronounced (compared to NDs and SMALPs), which likely reflects the small number of GM1 (average of 0.33 to 4.1 GM1 molecules) per disc. In comparison with the direct ESI-MS measurements, for 5, 10, and 20% PDs, the $K_{a,app}$ is within a factor of 2 to the measured K_a.

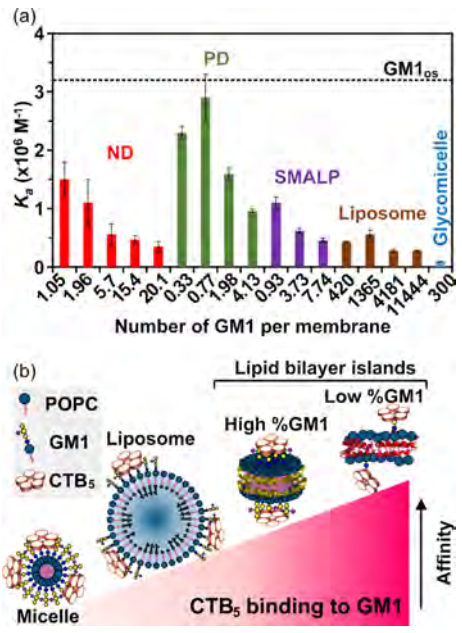

Figure 4. (a) Plot of intrinsic affinities (K_a) vs average number of GM1 per model membrane measured for CTB_5−GM1 binding with proxy ligand ESI-MS assay. Error bars correspond to one standard deviation. Dashed line: corresponding intrinsic K_a for the CTB_5−$GM1_{os}$ interaction (value taken from ref 38). (b) Illustration of the trend of K_a for CTB_5−GM1 binding in micelles, liposomes, and bilayer islands with high and low GM1 percentages.

https://doi.org/10.1021/acs.analchem.2c03067
Anal. Chem. XXXX, XXX, XXX−XXX

Factors Influencing GSL Affinity. Several important findings, which are summarized in Figure 4b, can be drawn from the aforementioned analysis of the K_a derived from the proxy ligand ESI-MS measurements. Most importantly, the GM1 PDs exhibit the highest affinity for CTB_5 and K_a that are similar to the intrinsic affinity of $GM1_{os}$. This suggests that the conformational space occupied by the GM1 head group in PDs resembles that of the free pentasaccharide in solution. The low % GM1 NDs and SMALPs exhibit somewhat weaker affinities but within a factor of ∼2 of those of the PDs. Both the NDs and SMALPs exhibit decreased binding with increasing % GM1, consistent with the occurrence of clustering. These results serve to highlight the importance of considering % GM1 when comparing affinities measured with different model membranes. Affinities measured for the GM1-containing liposomes are ∼10-fold weaker than that for the PDs, although relatively insensitive to % GM1. Given that liposomes are commonly viewed as surrogates for cell membranes, this observation raises the possibility that GBP−GSL binding is generally sub-optimal in authentic cellular environments. The GM1 glycomicelles exhibit the weakest affinity for CTB_5, ∼35-fold lower than that for $GM1_{os}$, consistent with steric effects due to GM1 packing and head group interactions. Finally, it is notable that the K_a are similar in magnitude to the $K_{a,app}$ measured for the 1−15% GM1 NDs, 3−30% GM1 liposomes, and 5−20% GM1 PDs. These results suggest that the direct ESI-MS measurements performed under conditions of high F, wherein all of the CTB_5 species detected originating from complexes with the model membranes in solution (and, thus, have similar response factors) can provide an estimate of affinity.

CONCLUSIONS

The results of this ESI-MS study of CTB_5−GM1, the first comparative investigation into how the nature of the model membrane affects GSL binding to a multisubunit GBP, provide timely guidance on designing quantitative binding experiments and highlight important considerations when comparing results obtained with different membrane systems. Affinity measurements performed with the proxy ligand ESI-MS suggest that bilayer islands (PDs, SMALPs, and NDs) with a low percentage GSL, wherein clustering is minimized, are ideal for assessing intrinsic strength of GBP−GSL interactions in the membrane environment. The affinities measured with liposomes are weaker (∼10-fold in the current study) than those of the low percentage GSL bilayer islands but relatively insensitive to the GSL content. This observation is likely due to the occurrence of extensive clustering resulting from the large number of GSLs in each particle. However, such sub-optimal binding (in terms of affinity) may reflect the situation in authentic cellular environments. The current findings also caution against the use of glycomicelles, which exhibit the lowest affinities, presumably due to steric hindrances resulting from the close GSL packing. Follow-up studies using other GBP−GSL systems (e.g., Siglec-ganglioside interactions) are now needed to test the generality of these findings.

The results of this work also expose limitations of ESI-MS analysis for quantifying GBP−GSL binding. Importantly, direct ESI-MS analysis generally does not provide an accurate representation of GSL binding due to the effects of non-uniform response factors, incomplete extraction of GBP−GSL complexes (from the membrane) in the gas phase, and the formation of nonspecific interactions (false positive) at high GSL concentrations. Additionally, for GBP capable of multivalent binding, certain concentration regimes (GBP and GSL/membrane) can lead to dramatic signal suppression. Although the origin of this previously unreported phenomenon has not been definitively established, it is suggested to arise from the formation of large aggregates, resulting from the binding of the GBP to multiple membrane particles.

ASSOCIATED CONTENT

Supporting Information

The Supporting Information is available free of charge at https://pubs.acs.org/doi/10.1021/acs.analchem.2c03067.

Preparation of the GM1-containing model membranes; quantifying GM1 contents in model membranes; proxy ligand ESI-MS assay; graphical representation of the possible interactions involving CTB_5, GM1, and L_{proxy}; $K_{a,app}$ for CTB_5−GM1 interactions; structures of the ganglioside, oligosaccharide, and lipids; representative ESI mass spectra; and titration plots (PDF)

AUTHOR INFORMATION

Corresponding Author

John S. Klassen − *Department of Chemistry, University of Alberta, Edmonton T6G 2G2 Alberta, Canada;* orcid.org/0000-0002-3389-7112; Phone: (780) 492-3501; Email: john.klassen@ualberta.ca; Fax: (780) 492-8231

Authors

Ling Han − *Department of Chemistry, University of Alberta, Edmonton T6G 2G2 Alberta, Canada;* orcid.org/0000-0002-3088-0374

Linh Nguyen − *Department of Chemistry, University of Alberta, Edmonton T6G 2G2 Alberta, Canada*

Edward N. Schmidt − *Department of Chemistry, University of Alberta, Edmonton T6G 2G2 Alberta, Canada*

Mansoore Esmaili − *Department of Biochemistry, University of Alberta, Edmonton T6G 2R3, Canada*

Elena N. Kitova − *Department of Chemistry, University of Alberta, Edmonton T6G 2G2 Alberta, Canada*

Michael Overduin − *Department of Biochemistry, University of Alberta, Edmonton T6G 2R3, Canada*

Matthew S. Macauley − *Department of Chemistry, University of Alberta, Edmonton T6G 2G2 Alberta, Canada; Department of Medical Microbiology and Immunology, University of Alberta, Edmonton T6G 2E1 Alberta, Canada;* orcid.org/0000-0003-4579-1048

Complete contact information is available at: https://pubs.acs.org/10.1021/acs.analchem.2c03067

Notes

The authors declare no competing financial interest.

ACKNOWLEDGMENTS

The authors acknowledge the Natural Sciences and Engineering Research Council of Canada, the Canada Foundation for Innovation, the Alberta Innovation and Advanced Education Research Capacity Program, and the Canadian Glycomics Network for generous funding. The authors thank Professor G. Privé (University of Toronto) for generously providing the saposin A.

https://doi.org/10.1021/acs.analchem.2c03067
Anal. Chem. XXXX, XXX, XXX−XXX

REFERENCES

(1) Varki, A.; Cummings, R. D.; Esko, J. D.; Stanley, P.; Hart, G. W.; Aebi, M.; Darvill, A. G.; Kinoshita, T.; Packer, N. H.; Prestegard, J. H.; Schnaar, R. L.; Seeberger, P. H. *Essentials of Glycobiology*, 3rd ed.; Cold Spring Harbor Laboratory Press: Cold Spring Harbor, New York, USA, 2017; p 823.
(2) Daniotti, J. L.; Lardone, R. D.; Vilcaes, A. A. *Front. Oncol.* **2016**, *5*, 300.
(3) Russo, D.; Parashuraman, S.; D'Angelo, G. *Int. J. Mol. Sci.* **2016**, *17*, 1732.
(4) Schnaar, R. L. *Arch. Biochem. Biophys.* **2004**, *426*, 163−172.
(5) Evans, S. V.; Roger MacKenzie, C. R. *J. Mol. Recognit.* **1999**, *12*, 155−168.
(6) Lingwood, C. A.; Manis, A.; Mahfoud, R.; Khan, F.; Binnington, B.; Mylvaganam, M. *Chem. Phys. Lipids* **2010**, *163*, 27−35.
(7) Shi, J.; Yang, T.; Kataoka, S.; Zhang, Y.; Diaz, A. J.; Cremer, P. S. *J. Am. Chem. Soc.* **2007**, *129*, 5954−5961.
(8) Hooper, N. M. *Curr. Biol.* **1998**, *8*, R114−R116.
(9) Nagafuku, M.; Kabayama, K.; Oka, D.; Kato, A.; Tani-ichi, S.; Shimada, Y.; Ohno-Iwashita, Y.; Yamasaki, S.; Saito, T.; Iwabuchi, K.; Hamaoka, T.; Inokuchi, J.-i.; Kosugi, A. *J. Biol. Chem.* **2003**, *278*, 51920−51927.
(10) Lingwood, D.; Binnington, B.; Róg, T.; Vattulainen, I.; Grzybek, M.; Coskun, U.; Lingwood, C. A.; Simons, K. *Nat. Chem. Biol.* **2011**, *7*, 260−262.
(11) Yahi, N.; Aulas, A.; Fantini, J. *PLoS One* **2010**, *5*, No. e9079.
(12) Han, L.; Morales, L. C.; Richards, M. R.; Kitova, E. N.; Sipione, S.; Klassen, J. S. *Anal. Chem.* **2017**, *89*, 9330−9338.
(13) Roy, J.; Pondenis, H.; Fan, T. M.; Das, A. *Biochemistry* **2015**, *54*, 6299−6302.
(14) Zhang, X.; Barraza, K. M.; Beauchamp, J. L. *Proc. Natl. Acad. Sci. U.S.A.* **2018**, *115*, 3255−3260.
(15) Chinnapen, D. J.; Hsieh, W. T.; te Welscher, Y. M.; Saslowsky, D. E.; Kaoutzani, L.; Brandsma, E.; D'Auria, L.; Park, H.; Wagner, J. S.; Drake, K. R.; Kang, M.; Benjamin, T.; Ullman, M. D.; Costello, C. E.; Kenworthy, A. K.; Baumgart, T.; Massol, R. H.; Lencer, W. I. *Dev. Cell* **2012**, *23*, 573−586.
(16) Chan, Y.-H. M.; Boxer, S. G. *Curr. Opin. Chem. Biol.* **2007**, *11*, 581−587.
(17) Castellana, E. T.; Cremer, P. S. *Surf. Sci. Rep.* **2006**, *61*, 429−444.
(18) Rydell, G. E.; Dahlin, A. B.; Hook, F.; Larson, G. *Glycobiology* **2009**, *19*, 1176−1184.
(19) Berselli, G. B.; Sarangi, N. K.; Gimenez, A. V.; Murphy, P. V.; Keyes, T. E. *Chem. Commun.* **2020**, *56*, 11251−11254.
(20) Zhao, H.; Lappalainen, P. *Mol. Biol. Cell* **2012**, *23*, 2823−2830.
(21) Williamson, M. P.; Suzuki, Y.; Bourne, N. T.; Asakura, T. *Biochem. J.* **2006**, *397*, 483−490.
(22) Zhang, S.; Berntsson, R. P. A.; Tepp, W. H.; Tao, L.; Johnson, E. A.; Stenmark, P.; Dong, M. *Nat. Commun.* **2017**, *8*, 1637.
(23) Schuler, M. A.; Denisov, I. G.; Sligar, S. G. *Methods Mol. Biol.* **2013**, *974*, 415−433.
(24) Kuthe, S. S.; Choudhari, Y. M.; Inamdar, N. N.; Mourya, V. *Des. Monomers Polym.* **2012**, *15*, 465−521.
(25) Sonnino, S.; Mauri, L.; Chigorno, V.; Prinetti, A. *Glycobiology* **2007**, *17*, 1R−13R.
(26) Prinetti, A.; Loberto, N.; Chigorno, V.; Sonnino, S. *Biochim. Biophys. Acta* **2009**, *1788*, 184−193.
(27) Ishitsuka, R.; Kobayashi, T. *Biochemistry* **2007**, *46*, 1495−1502.
(28) Ma, Y.; Sobkiv, I.; Gruzdys, V.; Zhang, H.; Sun, X.-L. *Anal. Bioanal. Chem.* **2012**, *404*, 51−58.
(29) Denisov, I. G.; Grinkova, Y. V.; Lazarides, A. A.; Sligar, S. G. *J. Am. Chem. Soc.* **2004**, *126*, 3477−3487.
(30) Olerinyova, A.; Sonn-Segev, A.; Gault, J.; Eichmann, C.; Schimpf, J.; Kopf, A. H.; Rudden, L. S. P.; Ashkinadze, D.; Bomba, R.; Frey, L.; Greenwald, J.; Degiacomi, M. T.; Steinhilper, R.; Killian, J. A.; Friedrich, T.; Riek, R.; Struwe, W. B.; Kukura, P. *Chem* **2021**, *7*, 224−236.
(31) Leney, A. C.; Rezaei Darestani, R. R.; Li, J.; Nikjah, S.; Kitova, E. N.; Zou, C.; Cairo, C. W.; Xiong, Z.; Privé, G. G.; Klassen, J. S. *Anal. Chem.* **2015**, *87*, 4402−4408.
(32) Han, L.; Kitova, E. N.; Li, J.; Nikjah, S.; Lin, H.; Pluvinage, B.; Boraston, A. B.; Klassen, J. S. *Anal. Chem.* **2015**, *87*, 4888−4896.
(33) Han, L.; Kitova, E. N.; Klassen, J. S. *J. Am. Soc. Mass Spectrom.* **2016**, *27*, 1878−1886.
(34) Han, L.; Xue, X.; Roy, R.; Kitova, E. N.; Zheng, R. B.; St-Pierre, Y.; Lowary, T. L.; Klassen, J. S. *Anal. Chem.* **2020**, *92*, 14189−14196.
(35) Bui, D. T.; Li, Z.; Kitov, P. I.; Han, L.; Kitova, E. N.; Fortier, M.; Fuselier, C.; Granger Joly de Boissel, P.; Chatenet, D.; Doucet, N.; Tompkins, S. M.; St-Pierre, Y.; Mahal, L. K.; Klassen, J. S. *ACS Cent. Sci.* **2022**, *8*, 963−974.
(36) Heim, J. B.; Hodnik, V.; Heggelund, J. E.; Anderluh, G.; Krengel, U. *Sci. Rep.* **2019**, *9*, 12243.
(37) Kitova, E. N.; El-Hawiet, A.; Schnier, P. D.; Klassen, J. S. *J. Am. Soc. Mass Spectrom.* **2012**, *23*, 431−441.
(38) Lin, H.; Kitova, E. N.; Klassen, J. S. *J. Am. Soc. Mass Spectrom.* **2014**, *25*, 104−110.
(39) Tharad, S.; Üzülmez, Ö.; Promdonkoy, B.; Toca-Herrera, J. L. *Int. J. Mol. Sci.* **2018**, *19*, 3819.
(40) Manna, M.; Róg, T.; Vattulainen, I. *Biochim. Biophys. Acta* **2014**, *1841*, 1130−1145.

https://doi.org/10.1021/acs.analchem.2c03067
Anal. Chem. XXXX, XXX, XXX−XXX